

# Identification of wave breaking from nearshore wave-by-wave records

K. Holand and H. Kalisch\*

*Department of Mathematics, University of Bergen, PO Box 7800, 5020 Bergen, Norway*

M. Bjørnstad

*The Norwegian Meteorological Institute, Allégaten 70, 5007 Bergen, Norway*

M. Streßer, M. Buckley, J. Horstmann, R. Carrasco-Alvarez, and M. Cysewski

*Institute of Coastal Ocean Dynamics,  
Helmholtz-Zentrum Hereon, Geesthacht, Germany*

V. Roeber

*Université de Pau et des Pays de l'Adour,  
chair HPC-Waves, SIAME, Anglet, France*

H.G. Frøysa

*Aqua Kompetanse AS, Havbruksparken,  
Storlavika 7, 7770 Flatanger, Norway*

(Dated: August 24, 2023)

## Abstract

Using data from a recent field campaign, we evaluate several breaking criteria with the goal of assessing the accuracy of these criteria in wave breaking detection. Two new criteria are also evaluated. An integral parameter is defined in terms of temporal wave trough area, and a differential parameter is defined in terms of maximum steepness of the crest front period. The criteria tested here are based solely on sea surface elevation derived from standard pressure gauge records. They identify breaking and non-breaking waves with an accuracy between 84% and 89% based on the examined field data.

---

\* Henrik.Kalisch@uib.edu

## I. INTRODUCTION

Wave breaking is the dominant mechanism of energy dissipation for surface waves in the oceans, and significant efforts have been made in the past decades to understand various aspects of breaking waves both in the coastal ocean and in the open sea [1]. After energy is transmitted from wind to waves during wave generation, waves can traverse vast distances in the world's oceans, eventually arriving at distant shores. As waves approach the beach, they tend to increase in height, steepen and eventually break near the beach. Depending on the beach slope and waveheight, this breaking can take a variety of shapes, and breaking waves on beaches were classified into spilling, plunging, collapsing and surging [2]. Due to its ubiquitous nature and large impact on surfzone dynamics, the understanding of breaking waves in shallow water is one of the most important aspects of coastal wave modeling and the design of coastal structures. Indeed, breaking waves have a major impact on sediment transport, beach erosion and exchange of nutrients and other suspended particles between the surfzone and the inner shelf [3, 4], and are also the driving force for the development of surfzone circulation patterns [4, 5].

In spite of the prominent role of wave breaking in the study of ocean waves, it is one of the least understood ocean surface processes [1, 6, 7]. As explained in [8], one of the main obstacles to advancing our understanding of wave breaking is the lack of a practical method for the detection of wave breaking. It is generally understood that a wave breaking event commences when the horizontal velocity of fluid particles near the wavecrest reach the same value as the wave velocity [3, 9], and expunged water particles slide down the wavefront in a spilling breaker, or the particle velocity eventually exceeds the crest velocity as water is rushed forward in an evolving jet [10–14]. So while the start of a breaking event may be defined as above, it is unclear whether such a point can actually be pinpointed in practice, especially in the case of incomplete information such as is often the case in field situations which is the main focus of the present work.

Indeed, the definition of breaking onset given above depends on the knowledge of particle velocities which are generally difficult to measure in field situations. As a consequence, indirect methods have been developed to detect wave breaking. In fact, a variety of wave breaking criteria based on wave properties such as wave steepness and asymmetry have been proposed. In the present note, we analyze recent field measurements [15] in the context of some of the existing breaking criteria based on wave geometry in order to determine which will work best as a diagnostic for breaking detection. The criteria tested include the traditional waveheight to depth threshold,

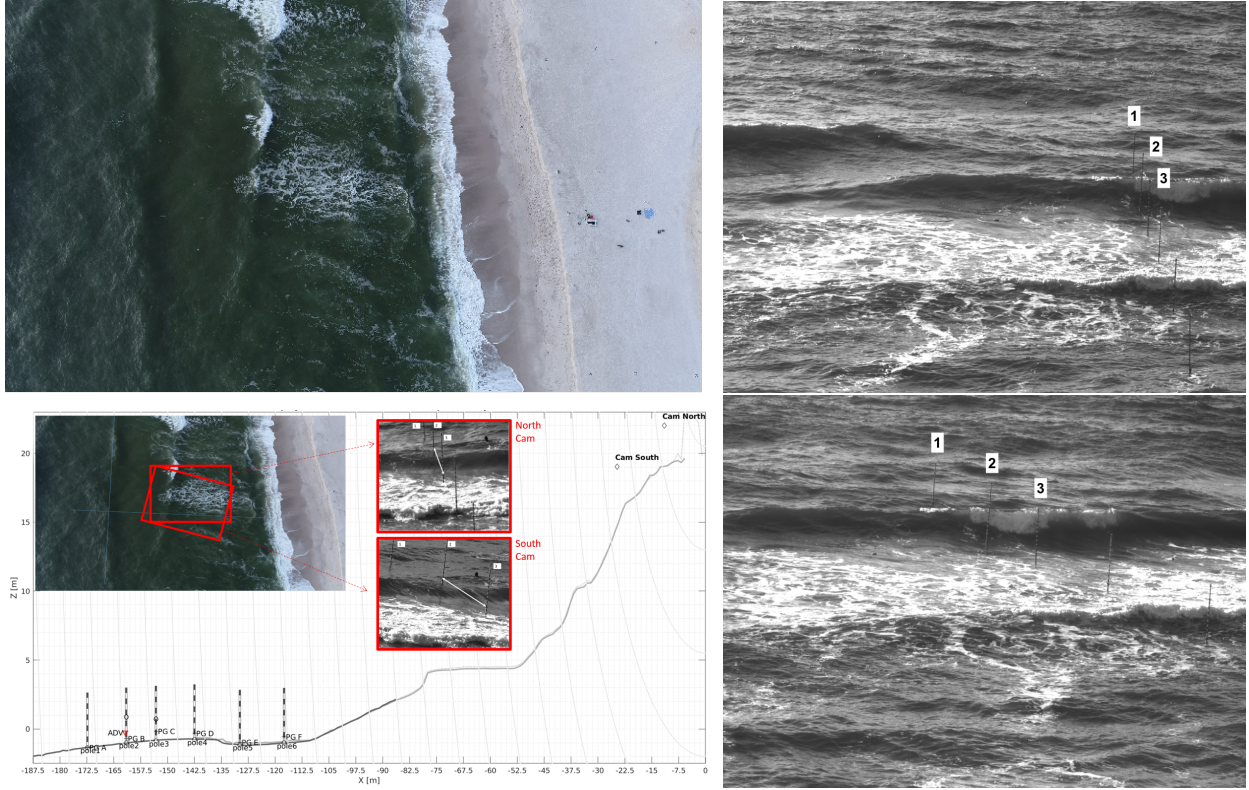


FIG. 1. Experimental setup: The upper left panel shows an aerial overview of the experimental site. The lower left panel shows the bathymetry, the arrangement of the poles and the Field of View (FOV) of the cameras. The right panels show a wider view of the poles for North Cam (upper) and South Cam (lower). The pressure signals used here are taken from the pressure gauges located at the bottom of poles 1, 2 and 3.

a number of different wave steepness measures as well as a new criterion based on an integral of the wave signal. It is found that the new criterion gives the best overall accuracy, but all criteria give acceptable levels of accuracy for determining whether a wave is breaking or not.

## II. BREAKING CRITERIA

Generally, there are three types of criteria used to determine the onset of wave breaking (for an in-depth overview, see for example [16, 17] and references therein). Geometric criteria predict wave breaking using the shape and more specifically the steepness and asymmetry of the free surface. Kinematic criteria probe for the violation of the kinematic free surface condition, essentially whether stagnation points appear at or near the wavecrest. Recent works have verified the accuracy of the kinematic criterion, in particular in shallow water situations [18, 19], but if the

kinematic criterion is to be used in a practical situation, estimates of phase or crest velocity have to be provided [20, 21]. Dynamic criteria are based either on accelerations exceeding some multiple of the gravitational acceleration [22, 23], or based on relations between energy flux and energy density [24, 25]. In fact, there are several physical mechanisms which can lead to wave breaking,

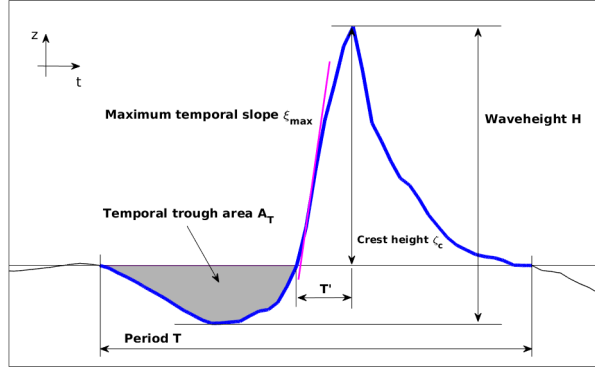


FIG. 2. Definition sketch of wave parameters used here. Waveheight  $H$ , crest height  $\zeta_c$ , wave period  $T$ , wave front period  $T'$ , temporal trough area  $A_T$  (units: meters·seconds) and maximum temporal slope  $\xi_{max}$  (units: meters / seconds).

for example crest instabilities in deep water [26], bottom forcing in coastal regions [27, 28], wind forcing [1] and forced discharge [29]. In general, one should distinguish between deep-water wave breaking (i.e. in the open ocean or on a lake, far from the shore) and shallow-water breaking, i.e. depth-induced breaking near the shore.

TABLE I. Wave breaking indicators. The indicator  $\kappa$  is defined in (1). The indicator  $\xi_{max}$  is defined in (2). The parameter  $\zeta_c$  is the crest height,  $T$  is the wave period,  $g$  is the gravitational acceleration,  $T'$  is the wave front period,  $H$  is the waveheight and  $h_0$  is the depth.

Criterion	Indicator	Units
Integral criterion	$\kappa$	
Maximum steepness	$\xi_{max}$	m/s
Steepness I	$\zeta_c/T'$	m/s
Steepness II	$\frac{\zeta_c}{(g/2\pi)T \cdot T'}$	
Steepness III	$H/T$	m/s
Waveheight/depth	$\gamma = H/h_0$	

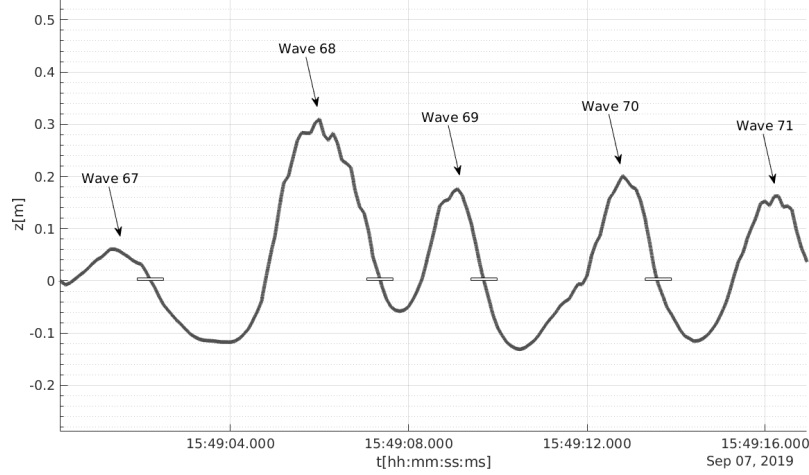


FIG. 3. Segmentation of the wave record. A zero down-crossing segmentation is applied to each wave record. In this figure, five waves in the record Cv48 at Pole 2 are shown (Wave 67 through Wave 71). The white bar designates the demarcation of two different wave events. For each wave in each record the basic parameters indicated in Figure 2 are found, and the six quantities delineated in Table 1 are computed.

Studies of wave breaking in shallow water have mostly focused on the breaker height following the pioneering work of McCowan [30] and later Munk [31] where the limiting relative waveheight for breaking solitary waves was found in terms of the waveheight to depth ratio  $H/h_0$ . The critical value of this ratio depends on a number of factors, and even for a flat bed, it is not entirely clear what the critical value should be [32]. In fact, many works have focused on empirical fits of the so-called breaker index the critical value of  $\gamma$  at which waves are expected to break. These studies are based on a number of dedicated laboratory and field studies with various bed slopes. For example, Madsen [33] defines a breaker index  $\gamma_b = 0.72(1 + 6.4m)$ , where  $m$  is the bed slope, and Battjes [34] defines  $\gamma_b = 1.062 + 0.137 \log(\xi_0)$  in terms of the surf similarity parameter  $\xi_0 = m\sqrt{L_0/H_0}$ , where  $H_0$  is the offshore waveheight and  $L_0$  is the offshore wavelength. An overview over much of the existing literature can be found in [35].

The main purpose of the present work is to test a number of wave breaking criteria as a simple diagnostic for deciding whether an individual wave in a given record is breaking or not. The diagnostic is based only on time series data of the free surface elevation. This time series could be obtained from a wave gauge or from a pressure sensor mounted in the fluid column or near the fluid bed. In this situation, the class of criteria based on wave shape appear to be most expedient. In some works which analyze data from laboratory experiments, the Phase-Time Method (PTM)

[18, 20, 36, 37], or the wavelet method [10, 38, 39] is used. Such an analysis would have to use the Hilbert transform to estimate phase and particle velocities [10] and would be inapplicable to field situations unless a special setup were to be used. In the present case, we focus on situations where common devices such as pressure gauges or single wave gauges are used, and the diagnostic should therefore use methods that require minimal postprocessing.

The criteria tested here are summarized in Table I. We test the traditional waveheight / depth criterion, as well as three different steepness criteria. For a given wave record, a wave-by-wave segmentation is applied, and each wave is assigned a number (see Figure 3). For each numbered wave, the basic quantities waveheight  $H$ , wave period  $T$  and crest height  $\zeta_c$  are found numerically (see Figure 2). In addition, the wave front period  $T'$ , i.e. the time between a zero-upcrossing until the wave crest is reached is found. From these quantities, the waveheight/depth ratio  $\gamma = H/h_0$ , and the three steepness parameters  $\zeta_c/T$ ,  $\frac{\zeta_c}{(g/2\pi)T \cdot T'}$  and  $H/T$  are computed for each wave in a given record.

In addition, we define a new parameter based on the size of the trough preceding a wave crest. This parameter is based on the observation that an extensive wave trough is often preceding a breaking wave. Hand in hand with a large trough goes a large steepness of the wave front, not necessarily as defined by the usual measures, but rather locally, so we also defined a new steepness criterion based on the maximum steepness (in terms of the temporal slope) of the wave front. We thus define wave breaking diagnostics on an integral measure, the size of the preceding trough (called *temporal trough area*  $A_T$ ) and a differential measure: the maximum slope of the crest front  $\xi_{max}$ . The exact definitions are as follows. We define the non-dimensional quantity

$$\kappa = \frac{H^2 \cdot A_T}{T \cdot h_0^3}, \quad (1)$$

where  $H$  is the waveheight,  $A_T$  is the temporal trough area (units m·s),  $T$  is the wave-by-wave period and  $h_0$  is the fluid depth. The temporal trough area is defined by  $A_T = \int_{t_{down}}^{t_{up}} |\eta(t)| dt$ , where  $t_{down}$  denotes the time of zero-down crossing defining the starting point of the the wave, and  $t_{up}$  denotes the up-crossing time immediately following  $t_{down}$  (see Figure 2) for a definition sketch. The maximum temporal slope is defined as

$$\xi_{max} = v_S \cdot \max_{t_i} \{ \eta(t_i) - \eta(t_{i-1}) \}, \quad (2)$$

where  $v_S$  is the sampling frequency and  $\eta(t_i)$  are free surface records between  $t_{up}$  and  $t_{down}$ . While the integral measure may have the advantage of being more stable due to an inclusion of the signal history, both measures work almost equally well for the wave records considered here.

### III. FIELD MEASUREMENTS

The measurements described here were obtained from a campaign that took place during 4-8 September 2019, on the western coast of Sylt, an island off the German North Sea Coast using a combination of both in situ and remote sensing measurement systems.

A long-range, high resolution four-camera stereo imaging system was specifically developed for this study. Two pairs of 5MP, global shutter CMOS digital cameras (Victorem 51B163-CX, IO Industries) were each fitted with Canon 50 mm and 400 mm lenses, respectively. The two camera pairs were placed on the ridge overlooking the beach, at a distance of 40m from one another. The four cameras were focused on a portion of water surface within the surf zone, located at an approximately distance of 150m from the cameras. A sketch of the instrument setup is provided in Figure 1.

Six graduated aluminum poles were jettied into the sand of an intertidal sandbar at low tide. The array of poles was aligned so as to be approximately perpendicular to the crests of incoming waves. The most seaward pole (Pole 1) was about 80 m from the shore, and the closest pole (Pole 6) was about 20 m from the shoreline. At the base of each pole, a pressure gauge measured absolute pressure at 10 Hz sampling frequency. The recorded pressure signal was subdivided into 10 minute data bursts and then transformed to surface excursion using the nonlinear method encapsulated in eq. (13) in [40]. This method has been found to be quite accurate, with the highest error of  $\sim 7\%$  at the wavecrest (see also [41]). Since the graduated poles were within the field of view of the stereo cameras (acquiring at 30 frames/second), these were also used as optical wave gauges in order to verify the nonlinear re-construction of the free surface.

### IV. DATA ANALYSIS

The data consists of pressure data and video frames of the sea surface at a shore in Sylt, Germany recorded in the period between 15:13:00 and 17:18:59 UTC on September 7th, 2019. In total, 903 wave events distributed over five data sets (datasets Cv46, Cv47, Cv48, Cv51 and Cv52) were analyzed. The waves were collocated at the first three poles (Pole 1, Pole 2 and Pole 3) with the corresponding time series from the pressure gauge records. The free surface elevation is reconstructed from the pressure data using the method explained in [40]. The sea surface time series is adjusted for tidal effects, and the approximate depth during one wave record is obtained

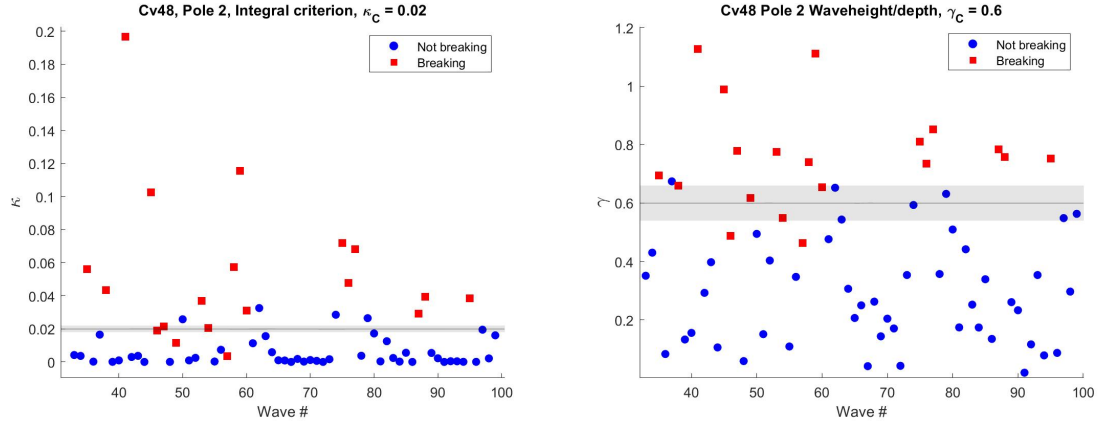


FIG. 4. Graphical representation of the identification of breaking and non-breaking waves for dataset Cv48 at Pole 2: The left panel shows evaluation of the integral criterion for breaking waves (red) and non-breaking waves (blue). The right panel shows the evaluation of the waveheight / depth criterion for breaking waves (red) and non-breaking waves (blue). The gray shaded area represents a 10% tolerance band for the critical value to take account of various errors in the measurements and imperfections in the data analysis such as the free surface reconstruction.

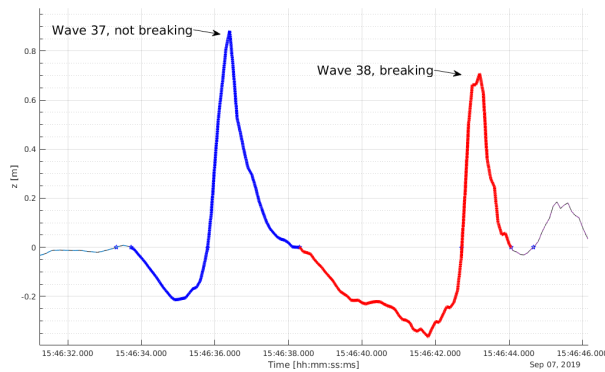


FIG. 5. Excerpt from data set Cv48 showing two wave profiles. The first wave (wave 37, shown in blue) is not breaking, while the second wave (wave 38, shown in red) is breaking. All traditional diagnostics based on wave shape fail to classify these waves accurately.

by averaging over the entire 10-minute record.

Wave conditions were monitored at an offshore buoy located in about 10m water depth. Conditions for significant waveheight were in the range 0.9 – 1m, peak period was in the range 6.25 – 6.7s, and peak direction was in the range 270 – 289°. The overarching aim here is to find a criterion for determining whether a given wave in the record is breaking or not, based solely



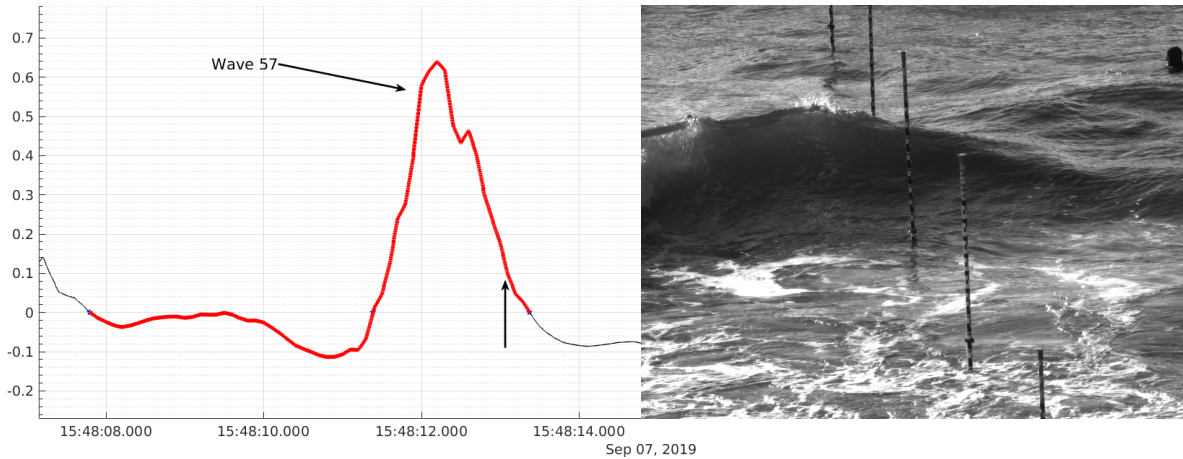


FIG. 6. One of the waves in the record Cv48 (Wave 57) which exhibited breaking at Pole 2, but which did not trigger either the waveheight/depth or the integral criterion. As can be seen in the frame from the North Cam, the reason appears to be that the wave is short-crested and coming in to shore at a slight angle, so that the correct signal history with regard to wave-breaking prediction is not available at Pole 2. The time series at pole 2 is shown in the left panel, and a single frame from the North Cam is shown in the right panel. The vertical arrow in the left panel denotes the time stamp from the frame in the right panel.

on the free surface time series derived from the pressure data. The visual images are only used for verification of the diagnostic.

Overall, at Pole 1, 20 out of 293, or 7% of waves are breaking. At Pole 2, 83 out of 300, or 28% of waves are actively breaking, and 75 out of 310 or 24% of waves are actively breaking at Pole 3. The water height usually decreases from Pole 1 to Pole 3 during the period of measurements which explains the different percentages of breaking waves for the different locations. At Pole 4 almost all waves have broken or are actively breaking, and at Pole 5 and 6, almost all waves have broken.

Wave breaking was defined by visual inspection, and a wave was counted as breaking at a given pole if breaking occurred in the vicinity of the pole. In some cases, ambiguities occurred, such as breaking of secondary crests riding on top of the main wave. If such an event was intermittent, lasting less than 1 second, this was not counted as a breaking wave.

In order to test the criteria under examination here, critical values for each diagnostic parameter must be found. The approach taken here was to calibrate the critical value of a diagnostic parameter using one of the 15 datasets (here we used Cv52 at Pole 2, but any other dataset could have been used). Once calibrated, the critical value was applied unchanged to the remaining datasets.

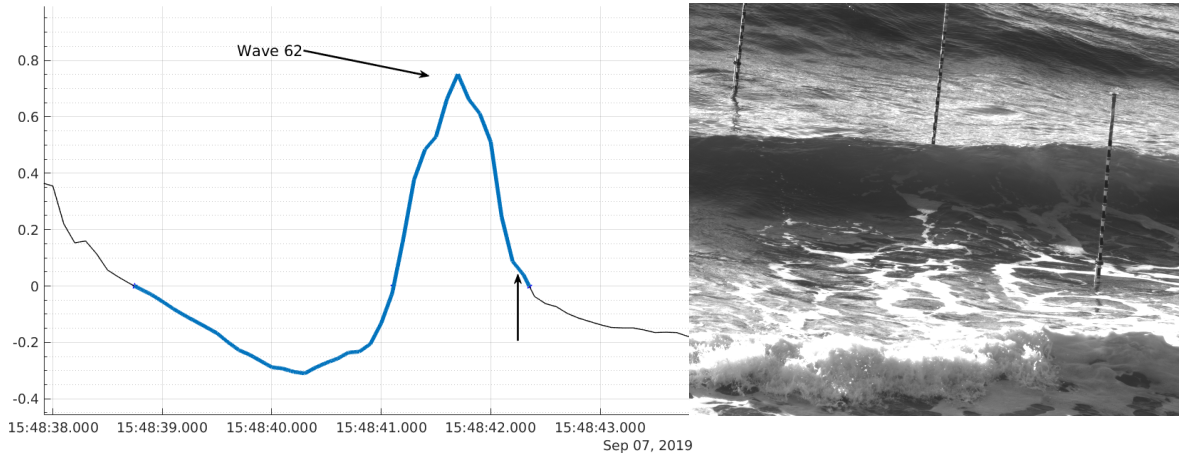


FIG. 7. One of the waves in the record Cv48 (Wave 62) which did not break at Pole 2, but which did trigger both criteria shown in Figure 4. The reason why breaking was retarded is not clear. Wind effects are a possibility. The time series at pole 2 is shown in the left panel, and a single frame from the North Cam is shown in the right panel. The vertical arrow in the left panel denotes the time stamp from the frame in the right panel.

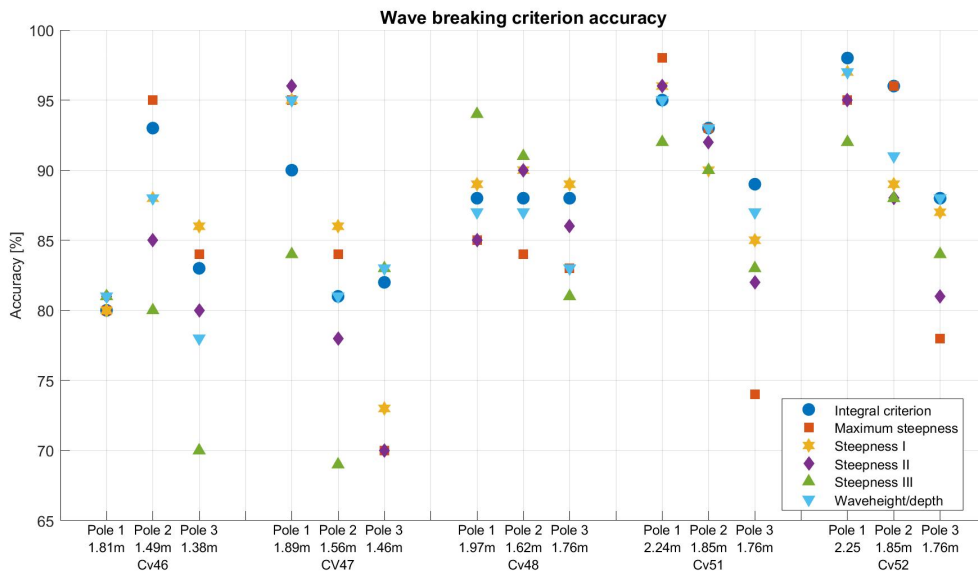


FIG. 8. Accuracy of the six different criteria in detecting breaking waves across all 15 datasets.

In order to account for the up to 7% error in the free surface reconstruction and various other small errors in the measurements, we incorporated a 10% tolerance band around the critical value of each diagnostic parameter. As can be clearly see in Figure 4, the accuracy in terms of share of correctly identified waves is rather stable with respect to this tolerance. For example, an increase

TABLE II. Accuracy of the six breaking detection criteria at each of the three poles. The overall accuracy shown in column 5 is given with an error which is determined by using a 10% error bar for the demarcation of individual wave events as shown in Figure 4.

Criterion	Pole 1	Pole 2	Pole 3	Overall accuracy
Integral criterion	91%	90%	87%	89% $\pm$ 1%
Max. steepness	92%	90%	77%	86% $\pm$ 1%
Steepness I	93%	90%	84%	87% $\pm$ 2%
Steepness II	92%	87%	81%	86% $\pm$ 3%
Steepness III	90%	85%	84%	86% $\pm$ 2%
Waveheight/depth	93%	88%	84%	88% $\pm$ 1%

from 10% to 15% would result in an increased error of only 1 – 2% in the overall accuracy.

Overall, the traditional criteria *Steepness I*, *Steepness II*, *Steepness III* and *Waveheight / depth* with the corresponding formulae given in Table I yield acceptable results for wave breaking identification. The best of these four criteria is the *Waveheight / depth* criterion with overall 88% accuracy across the 903 events studied here (see Table II). For a subset of wave events (Cv 48, Pole 2), the accuracy of the *Waveheight / depth* criterion is depicted in the right panel of Figure 4. The red squares signify waves which were visually inspected to be breaking at Pole 2 while the blue dots denote waves which are not breaking. The value of  $\gamma$  is indicated on the ordinate.

There are some constellations of waves where all of the traditional criteria give counter-intuitive results. Consider the two waves from record Cv48 shown in Figure 5. The wave on the left (Wave 37) is not breaking (indicated in blue) while the wave on the right (Wave 38) is breaking (indicated in red). For each of the traditional criteria, the value of the corresponding indicator is higher for Waves 37 than for Wave 38. The decisive property that appears to override all other metrics is the extensive wave trough preceding Wave 38. This deep trough essentially lowers the water depth, so that the succeeding wave crest is high enough relatively to the lower preceding depth to lead to wave breaking. This deep trough in combination with a still relatively large crest height leads to a steep wave front which is most easily detected with a local measure of steepness. These observations led us to define the *Integral criterion* (top line in Table I) and the *Maximum steepness criterion* (second row in Table I). As shown in Table II, the *Integral criterion*, represented by the indicator  $\kappa$  defined in (1) gives the highest overall accuracy, and also works evenly across various

observational records.

Each of the six criteria gives some false positives and false negatives. Two of such are shown in Figure 6 and Figure 7. For the wave shown in Figure 6, it is evident that it is short-crested, and the immediate elevation history at a single location (in this case Pole 2) is skewed, and will not allow an accurate classification of the wave with regards to breaking. The wave shown in Figure 7 triggered all breaking criteria, but did not break until it was too far from Pole 2 to be counted. It is not immediately obvious what caused the discrepancy.

## V. DISCUSSION AND OUTLOOK

In the present work, it has been demonstrated that breaking waves can be detected from nearshore wave-by-wave records with an 84% to 89% accuracy, at least based on the records from recent field measurements examined here (see Figure 8). Six criteria have been tested, and they all give acceptable results. A new integral criterion based on trough size of a wave has been put forward. While the new criterion gives the best overall performance, the improvement is too small to justify the additional complication of the temporal integration.

The breaking detection tested here works with a single wave gauge or pressure sensor. Environmental parameters such as precise bathymetry measurements, wind and current effects have purposely not been taken into account as we were aiming for a simple diagnostic which should give acceptable results in situations where such data are not available. Nevertheless, it would be interesting to test wave breaking detection based on these simple diagnostics in a controlled environment such as a wave flume or wave basin. Such a study might also cast more light onto why some false positives appear, for example Wave 62 shown in Figure 7 which triggered all criteria, but did not break close enough to Pole 2 to count as breaking.

The critical values of each diagnostic parameter was found using one of the 15 datasets, and then applied to the remaining records. It will be interesting to see whether some of these critical values hold also in other situations. For the critical waveheight-to-depth parameter value  $\gamma_c$ , a rather wide range of values has been suggested [42] (it appears however that most of the criteria have been validated only for laboratory data). Using the Madsen criterion with the bed slope of  $\sim 1 : 50$  at the experimental site, and the offshore wave conditions given by the buoy in 10m depth, a critical value of  $\sim 0.81$  is found, and the Battjes formula yields a critical value of  $\sim 0.78$ . Other works [32, 43] indicate a critical breaker height close to 0.6 which is similar to the

critical value found here during the calibration. As indicated already in [32], more field studies are required in order to draw any conclusions on whether there is a universally applicable breaker height definition.

Previous measurements and simultaneous visual observation are primarily available for deep-water situations (see for example [1, 44, 45]). In [44], it is suggested that geometric parameters such as local asymmetry and steepness cannot be used with confidence to determine whether a given surface record features a breaking or non-breaking wave. In contrast, we find that the criteria used here give the correct determination for close to 90% of all wave events. Previous studies successfully applying wave-by-wave properties of wave records in the context of wave breaking exist [8, 21], and partially motivated the current work.

While the present paper focuses on breaking detection, significant efforts have also been directed towards predicting wave breaking by identifying the point of breaking inception [25, 46]. Both methodologies are of importance for numerical ocean modeling. Breaking detection should be applied for preparing ocean data as input for numerical models while breaking prediction can be used to understand when numerical dissipation should be used to simulate wave breaking. In fact, recent works have illuminated the use of various wave-breaking criteria in Boussinesq-type models, and a number of different approaches have been implemented and tested [47–51]. While the waveheight-to-depth and steepness criteria have been mostly used as *breaking inception* criteria, here they have been indicated to work well as *detection criteria*.

## ACKNOWLEDGMENTS

We thank Jan Bødewadt and Jurij Stell for technical support. We acknowledge funding from the Research Council of Norway under grant no. 239033/F20, and from Bergen Universitetsfond,

MPB, JH, MS, MC, and RC wish to acknowledge from the Coasts in the Changing Earth System (PACES II) program of the Helmholtz Association, and support from the Deutsche Forschungsgemeinschaft (DFG, German Research Foundation, project number 274762653, Collaborative Research Centre TRR 181 *Energy Transfers in Atmosphere and Ocean*).

Volker Roeber acknowledges financial support from the I-SITE program *Energy & Environment Solutions* (E2S), the Communauté d’Agglomération Pays Basque (CAPB), and the Communauté Région Nouvelle Aquitaine (CRNA) for the chair position HPC-Waves and support from the European Union’s Horizon 2020 research and innovation programme under grant agreement no.

- 
- [1] A. Babanin, *Breaking and dissipation of ocean surface waves* (Cambridge University Press, 2011).
- [2] C. J. Galvin Jr, “Breaker type classification on three laboratory beaches,” *Journal of Geophysical Research* **73**, 3651–3659 (1968).
- [3] D. H. Peregrine, “Breaking waves on beaches,” *Annual Review of Fluid Mechanics* **15**, 149–178 (1983).
- [4] R. Davidson-Arnott, B. Bauer, and C. Houser, *Introduction to coastal processes and geomorphology* (Cambridge university press, 2019).
- [5] T. Scott, G. Masselink, M. J. Austin, and P. Russell, “Controls on macrotidal rip current circulation and hazard,” *Geomorphology* **214**, 198–215 (2014).
- [6] L. H. Holthuijsen, *Waves in oceanic and coastal waters* (Cambridge University Press, 2010).
- [7] A. Toffoli, A. Babanin, M. Onorato, and T. Waseda, “Maximum steepness of oceanic waves: Field and laboratory experiments,” *Geophysical Research Letters* **37** (2010).
- [8] D. Liberzon, A. Vreme, S. Knobler, and I. Bentwich, “Detection of breaking waves in single wave gauge records of surface elevation fluctuations,” *Journal of Atmospheric and Oceanic Technology* **36**, 1863–1879 (2019).
- [9] E. B. Thornton and R. Guza, “Transformation of wave height distribution,” *Journal of Geophysical Research: Oceans* **88**, 5925–5938 (1983).
- [10] S. R. Massel, *Ocean wave breaking and marine aerosol fluxes*, Vol. 38 (Springer Science & Business Media, 2007).
- [11] M. Banner and D. Peregrine, “Wave breaking in deep water,” *Annual Review of Fluid Mechanics* **25**, 373–397 (1993).
- [12] K.-A. Chang and P. L.-F. Liu, “Velocity, acceleration and vorticity under a breaking wave,” *Physics of Fluids* **10**, 327–329 (1998).
- [13] O. Kimmoun and H. Branger, “A particle image velocimetry investigation on laboratory surf-zone breaking waves over a sloping beach,” *Journal of Fluid Mechanics* **588**, 353–397 (2007).
- [14] P. Lubin, O. Kimmoun, F. Véron, and S. Glockner, “Discussion on instabilities in breaking waves: vortices, air-entrainment and droplet generation,” *European Journal of Mechanics-B/Fluids* **73**, 144–

156 (2019).

- [15] M. Bjørnestad, M. Buckley, H. Kalisch, M. Streßer, J. Horstmann, H. Frøysa, O. Ige, M. Cysewski, and R. Carrasco-Alvarez, “Lagrangian measurements of orbital velocities in the surf zone,” *Geophysical Research Letters* **48**, e2021GL095722 (2021).
- [16] C. H. Wu and H. Nepf, “Breaking criteria and energy losses for three-dimensional wave breaking,” *Journal of Geophysical Research: Oceans* **107**, 41–1 (2002).
- [17] M. Perlin, W. Choi, and Z. Tian, “Breaking waves in deep and intermediate waters,” *Annual Review of Fluid Mechanics* **45**, 115–145 (2013).
- [18] U. Itay and D. Liberzon, “Lagrangian kinematic criterion for the breaking of shoaling waves,” *Journal of Physical Oceanography* **47**, 827–833 (2017).
- [19] S. D. Hatland and H. Kalisch, “Wave breaking in undular bores generated by a moving weir,” *Physics of Fluids* **31**, 033601 (2019).
- [20] P. Stansell and C. MacFarlane, “Experimental investigation of wave breaking criteria based on wave phase speeds,” *Journal of Physical Oceanography* **32**, 1269–1283 (2002).
- [21] M. Postacchini and M. Brocchini, “A wave-by-wave analysis for the evaluation of the breaking-wave celerity,” *Applied Ocean Research* **46**, 15–27 (2014).
- [22] O. M. Phillips, “The equilibrium range in the spectrum of wind-generated waves,” *Journal of Fluid Mechanics* **4**, 426–434 (1958).
- [23] T. J. Bridges, “Wave breaking and the surface velocity field for three-dimensional water waves,” *Nonlinearity* **22**, 947 (2009).
- [24] J.-B. Song and M. L. Banner, “On determining the onset and strength of breaking for deep water waves. part i: Unforced irrotational wave groups,” *Journal of Physical Oceanography* **32**, 2541–2558 (2002).
- [25] X. Barthelemy, M. Banner, W. Peirson, F. Fedele, M. Allis, and F. Dias, “On a unified breaking onset threshold for gravity waves in deep and intermediate depth water,” *Journal of Fluid Mechanics* **841**, 463–488 (2018).
- [26] M. S. Longuet-Higgins and D. G. Dommermuth, “Crest instabilities of gravity waves. part 3. nonlinear development and breaking,” *Journal of Fluid Mechanics* **336**, 33–50 (1997).
- [27] J. T. Kirby and M. Derakhti, “Short-crested wave breaking,” *European Journal of Mechanics-B/Fluids* **73**, 100–111 (2019).
- [28] R. Briganti, G. Bellotti, R. Musumeci, E. Foti, and M. Brocchini, “Boussinesq modelling of breaking

- waves: description of turbulence,” in *Coastal Engineering 2004: (In 4 Volumes)* (World Scientific, 2005) pp. 402–414.
- [29] H. Favre, “Etude theorique et experimental des ondes de translation dans les canaux decouverts,” Dunod **150** (1935).
- [30] J. McCowan, “Xxxix. on the highest wave of permanent type,” *The London, Edinburgh, and Dublin Philosophical Magazine and Journal of Science* **38**, 351–358 (1894).
- [31] W. H. Munk, “The solitary wave theory and its application to surf problems,” *Annals of the New York Academy of Sciences* **51**, 376–424 (1949).
- [32] S. Massel, “On the largest wave height in water of constant depth,” *Ocean Engineering* **23**, 553–573 (1996).
- [33] O. S. Madsen, “Wave climate of the continental margin: Elements of its mathematical description,” *Marine Sediment Transport in Environmental Management* , 65–87 (1976).
- [34] J. A. Battjes, “Surf similarity,” in *Coastal Engineering 1974* (1974) pp. 466–480.
- [35] B. Robertson, K. Hall, R. Zytner, and I. Nistor, “Breaking waves: Review of characteristic relationships,” *Coastal Engineering Journal* **55**, 1350002 (2013).
- [36] N. E. Huang, S. R. Long, C.-C. Tung, M. A. Donelan, Y. Yuan, and R. J. Lai, “The local properties of ocean surface waves by the phase-time method,” *Geophysical Research Letters* **19**, 685–688 (1992).
- [37] O. M. Griffin, R. D. Peltzer, H. T. Wang, and W. W. Schultz, “Kinematic and dynamic evolution of deep water breaking waves,” *Journal of Geophysical Research: Oceans* **101**, 16515–16531 (1996).
- [38] S. Longo, “Turbulence under spilling breakers using discrete wavelets,” *Experiments in Fluids* **34**, 181–191 (2003).
- [39] S. Longo, “Vorticity and intermittency within the pre-breaking region of spilling breakers,” *Coastal Engineering* **56**, 285–296 (2009).
- [40] P. Bonneton, D. Lannes, K. Martins, and H. Michallet, “A nonlinear weakly dispersive method for recovering the elevation of irrotational surface waves from pressure measurements,” *Coastal Engineering* **138**, 1–8 (2018).
- [41] A. Mouragues, P. Bonneton, D. Lannes, B. Castelle, and V. Marieu, “Field data-based evaluation of methods for recovering surface wave elevation from pressure measurements,” *Coastal Engineering* **150**, 147–159 (2019).
- [42] B. Robertson, K. Hall, I. Nistor, R. Zytner, and C. Storlazzi, “Remote sensing of irregular breaking wave parameters in field conditions,” *Journal of Coastal Research* **31**, 348–363 (2015).



- [43] M. K. Brun and H. Kalisch, “Convective wave breaking in the kdv equation,” *Analysis and Mathematical Physics* **8**, 57–75 (2018).
- [44] L. Holthuijsen and T. Herbers, “Statistics of breaking waves observed as whitecaps in the open sea,” *Journal of Physical Oceanography* **16**, 290–297 (1986).
- [45] K. B. Katsaros and S. S. Ataktürk, “Dependence of wave-breaking statistics on wind stress and wave development,” in *Breaking Waves: IUTAM Symposium Sydney, Australia 1991* (Springer, 1992) pp. 119–132.
- [46] M. Derakhti, J. T. Kirby, M. L. Banner, S. T. Grilli, and J. Thomson, “A unified breaking onset criterion for surface gravity water waves in arbitrary depth,” *Journal of Geophysical Research: Oceans* **125**, e2019JC015886 (2020).
- [47] V. Roeber, K. F. Cheung, and M. H. Kobayashi, “Shock-capturing boussinesq-type model for nearshore wave processes,” *Coastal Engineering* **57**, 407–423 (2010).
- [48] M. Bjørkavåg and H. Kalisch, “Wave breaking in Boussinesq models for undular bores,” *Physics Letters A* **375**, 1570–1578 (2011).
- [49] M. Tonelli and M. Petti, “Simulation of wave breaking over complex bathymetries by a boussinesq model,” *Journal of Hydraulic Research* **49**, 473–486 (2011).
- [50] M. Tissier, P. Bonneton, F. Marche, F. Chazel, and D. Lannes, “A new approach to handle wave breaking in fully non-linear boussinesq models,” *Coastal Engineering* **67**, 54–66 (2012).
- [51] P. Bacigaluppi, M. Ricchiuto, and P. Bonneton, “Implementation and evaluation of breaking detection criteria for a hybrid boussinesq model,” *Water Waves* **2**, 207–241 (2020).